Paper I 6

DIGITAL RECTIFICATION OF ERTS MULTISPECTRAL IMAGERY

Samuel S. Rifman, *TRW Systems Group, Redondo Beach, California*

ABSTRACT

Rectified ERTS multispectral imagery have been produced utilizing all digital techniques, as the first step toward producing precision corrected imagery. Errors arising from attitude and ephemeris sources have been corrected, and the resultant image is represented in a meter/meter mapping utilizing an intensity "resampling" technique. Early results from available data indicate negligible degradation of the photometric and resolution properties of the source data as a consequence of the geometric correction process. Work utilizing ground control points to produce precision rectified imagery, and including photometric corrections resulting from available sensor calibration data, is currently in progress.

I. INTRODUCTION

The production of precision processed ERTS imagery requires both precision rectification (correction of spatial distortions) of the bulk image data, as well as photometric correction of intensity values using sensor calibration data. In performing the respective corrections to the bulk imagery, it is necessary to account for a number of diverse error sources peculiar to the two sensor systems carried aboard ERTS: the three Return Beam Vidicon (RBV) cameras and the Multispectral Scanner (MSS). It is also necessary to compensate for errors external to the sensors, arising from spacecraft attitude, ephemeris and earth curvature.

In general, the problem of producing precision corrected images involves: first, the modeling of error sources that are to be corrected, and the development of techniques for accomplishing the corrections; and second, the implementation of a suitable algorithm for producing the corrected image. The emphasis of this paper will be on the second problem, with respect to some of the techniques and problems associated with the production of corrected imagery. Furthermore, because of the convenience and precision associated with the manipulation of imagery in a digital form, this paper is concerned with the problem of precision processing of imagery by purely digital techniques.

The well-known advantages of digital processing methods with respect to precision and permanence lend themselves directly to the task of generating precision digital image products for use by current and future investigators (for example, in scene/scene comparisons performed in the course of change discrimination studies). Advances in computer systems (see Reference 1 for a recent review article) have been matched recently by advances in algorithm development to make possible all-digital precision image processing, with moderate computer times. Following a

discussion of error sources, examples of ERTS-1 MSS imagery rectified by all-digital techniques at TRW Systems Group will be presented, together with a discussion of the relative merits of several algorithms utilized to produce the imagery. Extensions of these results to processing via modern mini-computers will also be indicated.

II. MSS ERROR SOURCES

Users of precision rectified ERTS imagery generally require that the products be represented in a rectangular cartesian coordinate system, i.e., that linear distance on the ground be faithfully represented in the imagery, free of errors arising within the sensor system, the spacecraft attitude and ephemeris, earth rotation and earth curvature.

Shown in Figure 1 (Reference 2), is a schematic diagram of the MSS sensor* carried aboard ERTS-1. The four band (0.5 - 1.1μm) sensor scans 185 Km wide cross-track swaths (each composed of 6 scan lines) by means of an oscillating planar mirror, which images all four bands simultaneously. The four bands are thus inherently spatially registered. The instantaneous field-of-view (IFOV) of a single sensor element is approximately 79m square on the ground from the nominal satellite altitude.
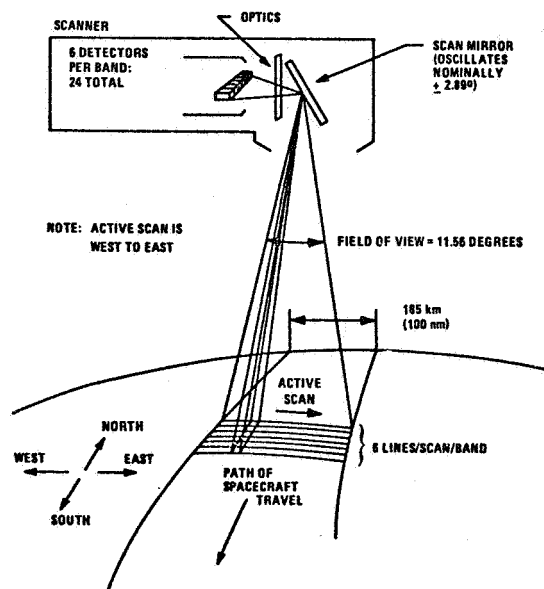

Figure 1. MSS Scanning Arrangement

---

* Due to the early cessation of data collection from the ERTS-1 RBV system, no discussion of error sources or correction algorithms for that sensor is included here. It is noted, however, that many algorithms developed for the MSS sensor are similar to those for the RBV sensor and have been included in the software package developed for the RBV system.

Each MSS bulk image represents 2340 individual active scan lines (scanned 6 at a time), obtained during approximately 28.6 sec. of "picture time." The mirror scan/retrace time is 73.42 ms (per 6 scan lines) and the sampling interval is 9.95 µs, so that the center/center cross-track separation of adjacent IFOV's is about 57m (nearly 30% overlap between adjacent samples).

It can now be seen that the following errors contribute in various degrees to spatial distortion in the bulk imagery: (1) scan nonlinearity, starting time jitter, repeatability, etc.; (2) change in spacecraft attitude during a picture time; (3) change in spacecraft altitude during the picture time; (4) earth curvature, a function of latitude; and (5) earth rotation, a function of latitude.

Inherent sensor errors (1) are given as $\pm$ 26m rms by Reference 2, and are therefore small and can be ignored. The bulk image data, however, have been scan length corrected to compensate for small variations in the number of samples per scan group. When this correction algorithm becomes available, it is anticipated that this small error can be corrected by means of the resampling algorithm described later.

Spacecraft attitude motion during picture scan can cause the groups of six lines to be non-parallel to each other when projected on to the ground. This effect manifests itself as a non-linear scale distortion throughout the bulk image. Change in spacecraft attitude during the picture time can also cause a small change in scale throughout the image. Earth curvature causes a scale change in the scan direction. Finally, earth rotation produces a $\sim$3° skew distortion (at $\sim$ 35-40°N latitude) in the image, essentially in the scan direction. The largest sources of error are due to the earth rotation, and the unequal number of scan lines (2340) and samples/scan ($\sim$ 3230) for a scene nominally 185 Km square.

III. IMAGE RECTIFICATION

The MSS rectification software developed by TRW currently corrects for error sources (2) – (5) using image annotation tape (BIAT or DIAT) data. In addition, a correction is made for the boresighting error, the difference between image format center (0° mirror scan) and spacecraft nadir. Provision has also been made for the inclusion of ground control points (GCP's), which are accurately measured locations of identifiable features that are used for precision image rectification. However, due to delays in obtaining the required data (bulk image tape, annotation data, and bulk imagery) for the target sites selected, it was not possible to include this refinement in the initial group of processed imagery. The ability to utilize GCP data has been verified for other scenes for which annotation data were not available.

The software developed for the precision correction of ERTS-1 imagery is shown in the functional flow diagram of Figure 2. Bulk image data is reformatted to produce a single tape with separate files containing data for each spectral band. At the same time regions called "neighborhoods" surrounding GCP locations are extracted, and are searched subsequently to precisely determine locations of GCP's within the image, using a reference library of GCP's. The GCP location data is used by a Kalman filter to refine the spacecraft attitude.
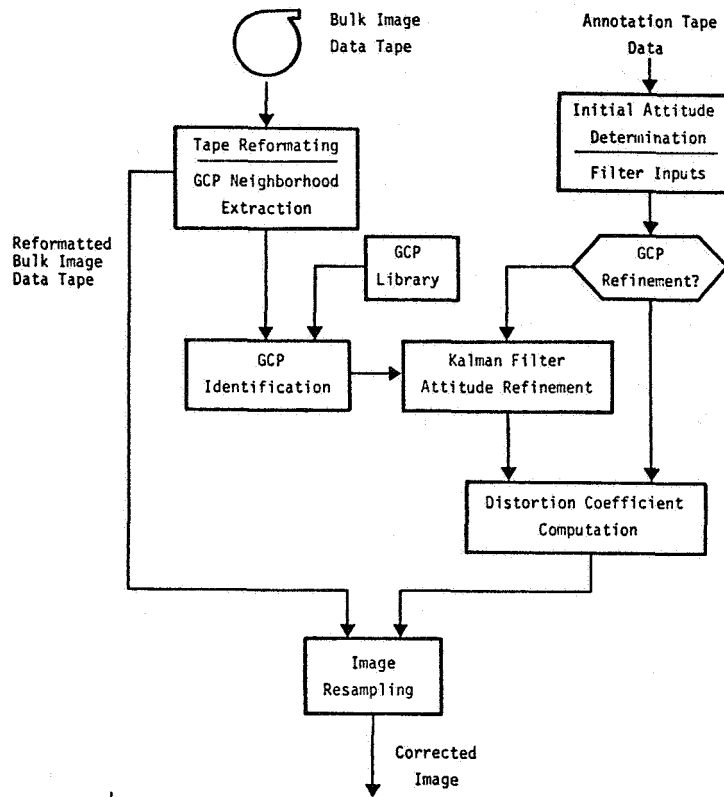
Figure 2. Precision Correction Software Schematic

Making use of the refined (or initial) attitude determination, distortion coefficients are computed which define the amounts by which the bulk image must be distorted so as to produce a rectified image, i.e., one which is linear in meter/meter coordinates. The computation of the coefficients is accomplished by mapping a small number of image locations, called "pseudo reseau points," to the final meter/meter coordinate system, taking into account the mirror scan, spacecraft attitude and ephemeris, earth rotation and earth curvature. Distortion coefficients are then defined for blocks of four pseudo reseaux, assuming a bilinear spatial distortion model (which introduces negligible errors compared to the self-consistency errors if there are enough pseudo reseaux).

The distortion coefficients thus determined are then transmitted to the resampling software, which processes the reformatted image tape so as to produce the final corrected image, including (if desired) photometric correction as well. The resampling code ensures that the output image contains the desired number of lines and samples/line, with uniform spacing of samples and lines.

1134

An appreciation of the resampling problem may be gained by refer-
ring to Figure 3. Essentially the bulk image (array of x's) in Figure
3-a is distorted to the coordinate system of the corrected scene image
(filled in zeros) of Figure 3-b, as a result of the geometric correction
algorithms outlined in Figure 2. It then becomes necessary to define
new values of data at the positions of the filled zeros, in terms of the
given values at the position of the x's. This procedure is called
interpolation.

There are several interpolation methods which provide a regular
grid of lines and samples in the output corrected image, given a cor-
rected image of unevenly spaced lines and samples. The simplest approach
involves selecting the "nearest neighbor," as illustrated in Figure 4-a.
In this approach, the data value of the sample (sometimes called a pixel)
in the irregular array of the corrected image closest to the location of
a pixel in the desired regular grid is used for the value of the regular
grid point. Clearly, the intensity values resulting from this interpola-
tion scheme correspond to true pixel locations that can be as much as
$\pm$ 1/2 a spacing in error (in the regular grid). On the other hand, the
computational requirements of this method are relatively modest, inasmuch
as only one data value is required to determine the resampled data value.
This results in relatively short running times.

An alternate method for image resampling is called bilinear inter-
polation (Figure 4-b), which utilizes a bilinear combination of the four
closest pixel values in the irregular grid of the corrected image to com-
pute a resampled data point. This method involves more computational time,
and may result in a small loss of image resolution, due to the smoothing
nature of the bilinear interpolation. On the other hand, the pixel "jitter"
(one spacing offsets) at rapidly changing contours associated with the
nearest neighbor scheme is avoided.

Cubic convolution resampling is an approximation to ideal sinx/x
resampling. When the image content is band limited (in the spatial
frequency domain), the ideal reconstruction of sampled data is of the
form

$$I(x_i) = \sum_{x_K} I(x_K) \ f(x_i - x_K),$$

wherein f(x) is of the form sinx/x, and I is the function being resampled.
By fitting a cubic polynomial to f (and imposing conditions for continuity,
cutoff, etc.), a unique function results. Such a function is given in
Figure 4-c for a cutoff at x=2, which utilizes 16 data values to compute
one resampled data point. Because the convolution method most closely
resembles the ideal resampling algorithm, it is expected to yield the
most satisfactory results, with respect to resolution and fidelity, com-
pared to nearest neighbor and bilinear interpolation. That is, the slope
and magnitude continuity properties of cubic convolution are superior
to the bilinear and nearest neighbor algorithms, by virtue of the more
global nature of the data values used to produce a resampled point.

IV. RESULTS

First results of the rectification process described in Section III

(a) Nearest Neighbor Interpolation

(b) Bilinear Interpolation
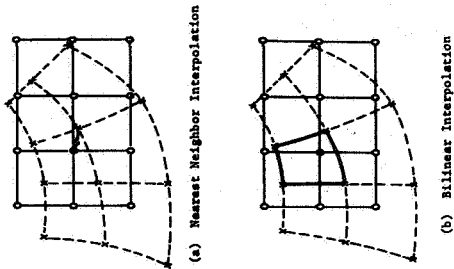
$$f(x) = 1 - 2 |x|^2 + |x|^3 \qquad 0 \le |x| \le 1$$
$$4 - 8 |x| + 5 |x|^2 - |x|^3 \qquad 1 \le |x| \le 2$$
$$0 \qquad 2 \le |x|$$

(c) Cubic Convolution Function

Figure 4. Three Possible Resampling Algorithms. Circles denote uniform pixel locations in the output, corrected image. x's denote the irregular grid of pixels (in the corrected image), derived by straightforward corrective distortions to the input bulk image. Filled in zero is a typical pixel, the value of which is to be interpolated.
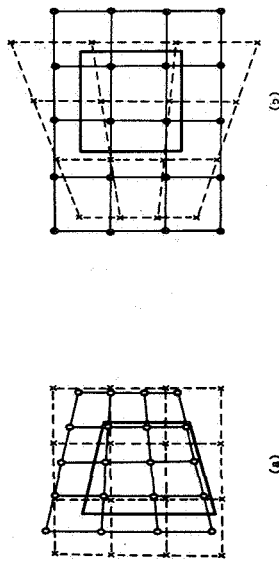

(b)

(a)

Figure 3. Resampling Problem. (a) x's denote bulk image sample locations, with respect to which the trapezoidal shaped object is imaged; (b) Filled zeros denote image sample locations in the final corrected digital image, with respect to which the rectified object is seen as a true square. The unfilled zeros in (a) represent the mapped locations of the desired image pixel locations, the values of which must be found by using an interpolation algorithm applied to the values at the x-locations. Alternatively, in the (b) system, x's denote mapped input (bulk) pixel locations in the corrected image system, which are used in conjunction with an interpolation algorithm to define the values at the filled zero locations.

were obtained for the scene 1057-18712-7 (San Francisco Bay and Monterey Bay) and involve the nearest neighbor and bilinear resampling algorithms. The convolution algorithm was developed prior to this study and converted to the ERTS data requirements. However, ERTS images were processed by means of this algorithm at too late a date to be included here.

Figure 5 shows the entire scene, reproduced from a bulk image transparency supplied by NASA/GSFC. Note that the bulk image has been corrected for the unequal number of lines and samples/line in the bulk data, as well as earth rotation. Figure 6* shows a detail taken from the upper left corner of the image, reconstructed** from the unrectified bulk image data tape supplied by NASA. The area shown is approximately 45 Km across and 120 Km long.

A rectified image corresponding to the detail in Figure 6 is given in Figure 7, utilizing the nearest neighbor interpolation algorithm. The area shown is 46.25 Km x 73.9 Km, and is aligned parallel to the spacecraft ground track. Note the steps occurring on the left edge of the image, corresponding to the successive one pixel increments associated with nearest neighbor interpolation. Careful examination of the image reveals a number of areas for which this pixel jitter is observed, and which is particularly evident for such high contrast regions as those containing a boundary between land and water. Thus, for example, note the bends in the San Antonio Creek, leading off from the WNW corner of San Pablo Bay, located in the upper middle of Figure 7 (portions of San Francisco Bay are located in the lower right of the figure, but are hidden by cloud cover).

Figure 8 shows the same scene as Figure 7, but using bilinear interpolation instead of nearest neighbor interpolation. Note the straight line appearance of the left edge of the image, in contrast to Figure 7. Note also that the bends in the San Antonio Creek are cleaner. On the other hand, note the slight resolution degradation for the complex of roads (including Interstate 80) north of Carquinez Strait, and east of Mare Island and the Napa River, compared with Figure 7. This degradation is expected by virtue of the smoothing effect of bilinear interpolation, and is absent in nearest neighbor interpolation.

It is worthwhile emphasizing here that the rectification processing was accomplished by all digital processing methods, utilizing input digital imagery. In contrast to this, bulk imagery (such as in Figure 5) is produced at the NASA Data Processing Facility by converting digital data to analogue data, and then utilizing an Electron Beam Recorder to rescan the image onto the output film.

In addition, it is useful to point out the required processing times for the production of rectified imagery. The images shown in Figures 7 and 8 were processed on a CDC 6400. Exclusive of the resampling portion, the required processing time was less than 10 seconds. In-

---

* Inasmuch as this paper is concerned with image rectification, the pictures included here have been slightly contrast-enhanced so as to bring out the image detail more clearly.

** The reconstructed images were produced from the corrected image tapes by photographing directly a high resolution CRT face, at the Jet Propulsion Laboratory's Image Processing Laboratory. The bright area in the upper left corner is a result of the reconstruction process, and is not in the corrected image data.
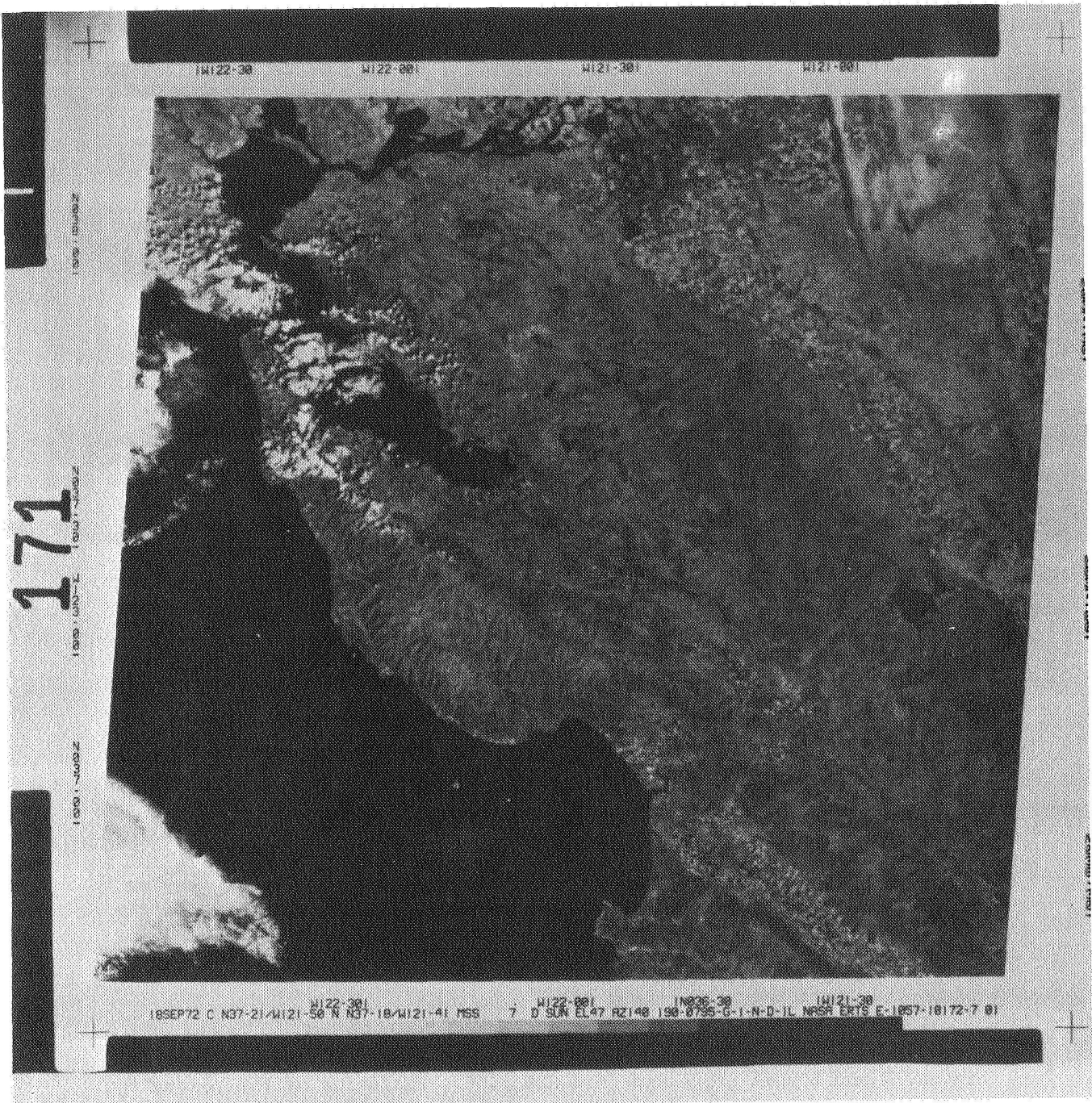
Figure 5. Reproduction of Scene 1057-18172-7 Bulk Image Print.
The image has been corrected for the difference in the number
of pixels/line and the number of lines, and has also been
corrected for earth rotation (skew).

1138

Figure 6. Reconstruction of Bulk Image Tape. This detail is taken from the upper left corner of Figure 5, and shows San Pablo Bay in the upper middle, and Port of San Francisco Bay in the right middle, partially obscured by cloud cover.
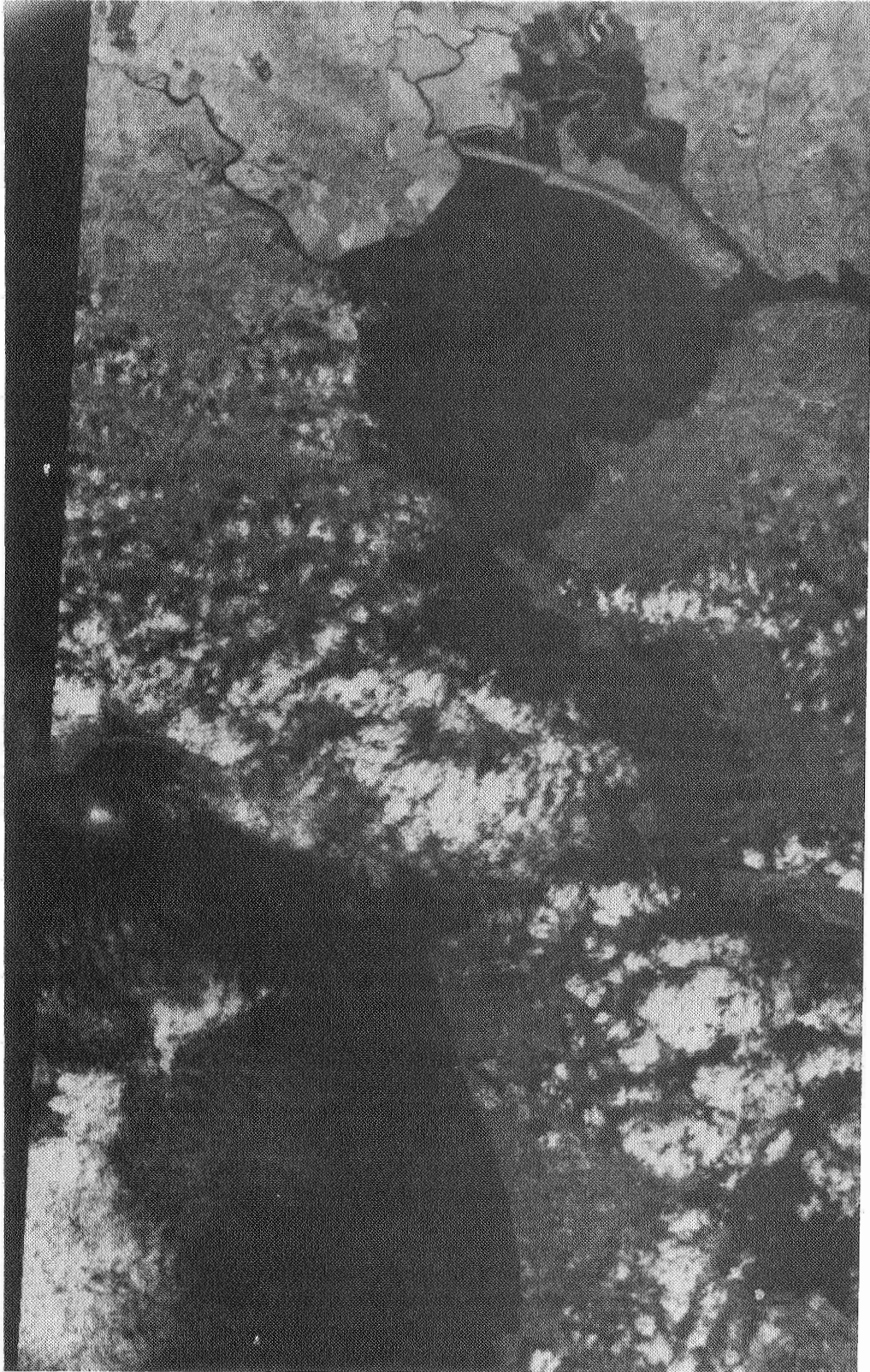
Figure 7. Reconstruction of a Portion of Figure 6 After
Rectification, Using Nearest Neighbor Interpolation. Note
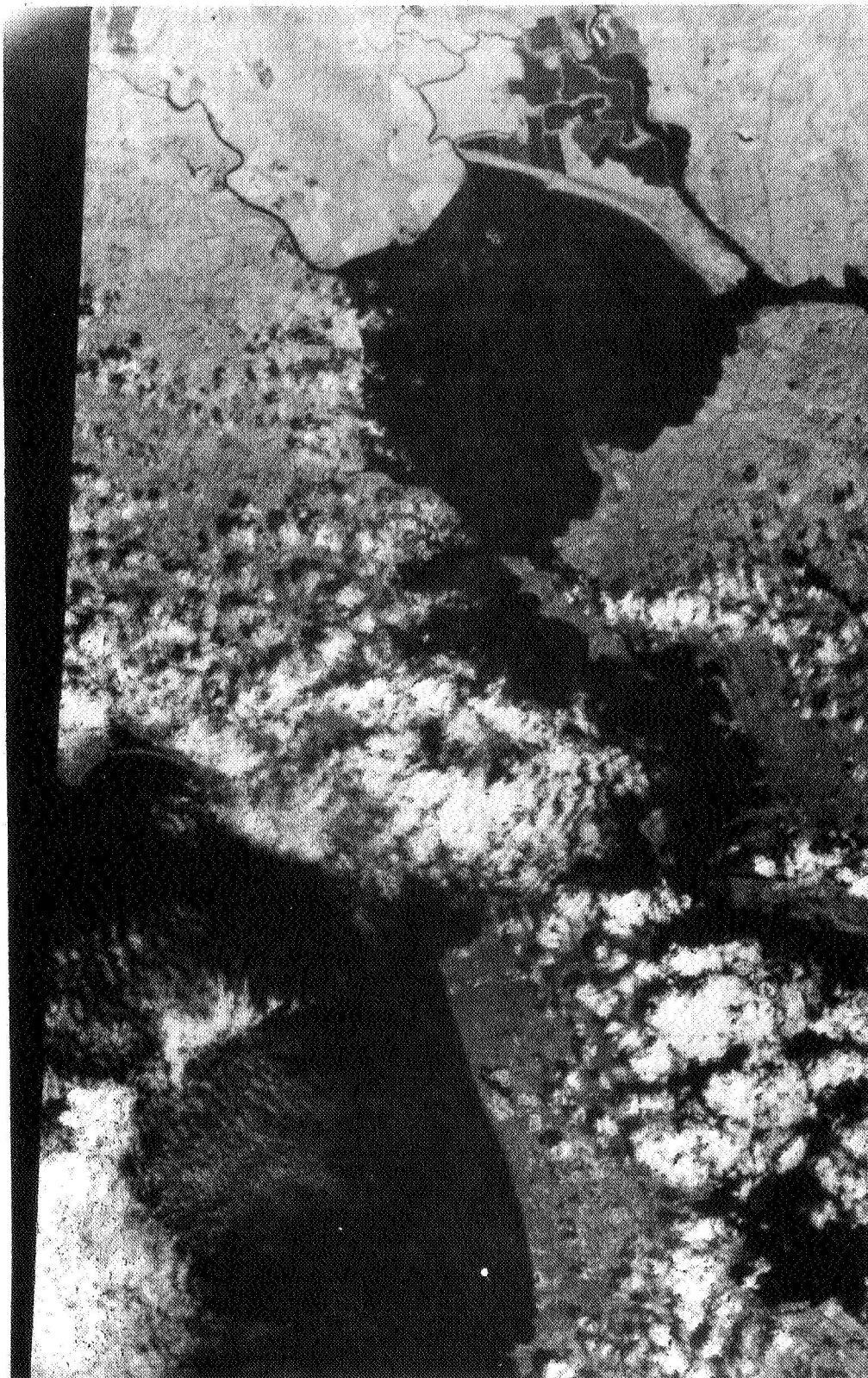the one pixel offsets on the left edge of the rectified image.

Figure 8. Reconstruction of a Portion of Figure 6 After
Rectification, Using Bilinear Interpolation. Note the smooth
appearance of the left edge of the rectified image, in
comparison to Figure 7.

cluding GCP processing, the time required is of the order of a minute or two (depending on the number of GCP's). The most time consuming portion is the resampling algorithm, which requires approximately 52 seconds of CPU time per 10^6 pixels for bilinear interpolation. Cubic convolution requires approximately 110 seconds. In contrast, extrapolations to a PDP-11/45 minicomputer indicate 28 seconds of CPU (per 10^6 pixels) would be required for bilinear interpolation, or approximately 60 seconds of CPU for cubic convolution.

V. CONCLUSIONS

Early results have been presented for the digital rectification of ERTS imagery. Two interpolation algorithms were employed to produce the final corrected imagery included here. It was shown that small errors ($\sim$ 1 pixel, or < 60 m) result from the resampling process, for only modest CPU requirements. Nearest neighbor interpolation produces ± 1/2 pixel jitter (horizontal and vertical) which is evident in regions of high contrast. On the other hand, bilinear interpolation supplants the single pixel offsets with smooth transitions, but at the price of somewhat larger CPU times and some slight resolution degradation. It is anticipated that the cubic convolution resampling algorithm will combine the best properties of nearest neighbor and bilinear interpolation, with only modest additional CPU requirements over those for bilinear resampling. In fact, processing speeds in general have reached the point at which it is now possible to consider processing all ERTS imagery by digital methods alone.

Acknowledgement

The author gratefully acknowledges the assistance of Mr. John Morecroft of the Image Processing Laboratory of JPL in the production of negatives from our digital image tapes.

References

1. G. Nagy, "Digital Image-Processing Activities in Remote Sensing for Earth Resources," Proc. IEEE 60, 1177-1200 (October 1972). This paper is included in the Special Issue on Digital Pattern Recognition.

2. Earth Resources Technology Satellite Data Users Handbook, General Electric Document No. 71SD4249 (September 15, 1971; Revised November 17, 1972).